FP7 PROGRAMME

DORIS - Ground Deformations Risk Scenarios:
an Advanced Assessment Service

GRANT AGREEMENT NO. 242212
COLLABORATIVE PROJECT
START DATE: OCTOBER 1ST 2010

WP3 – Value added research and technology development

DELIVERABLE No. D3.4
Integrated use of space-borne and ground-based SAR data

DOCUMENT INFORMATION

Acronym of lead partner for the deliverable	UNIFI
Work package	WP 3
Contractual date of delivery	Month 24
Date of delivery	September 2012
Nature	O
Dissemination level	PP

Document Responsible	Nicola Casagli (UNIFI)
Authors	Sandro Moretti (UNIFI) Chiara Del Ventisette (UNIFI) Federica Bardi (UNIFI) Federico Di Traglia (UNIFI) Andrea Ciampalini (UNIFI) Tazio Strozzi (GAMMA) Gerardo Herrera (IGME) Jose Fernández Merodo (IGME)

Release	1
Version	2
Date	October 2012

REFERENCE DOCUMENTS

DR-1	Annex I - Description of Work of DORIS – "Ground Deformations Risk Scenarios: an Advanced Assessment Service"
DR-2	Deliverable 3.3 - "Exploitation of multi-frequency InSAR products"
DR-3	Deliverable 3.5 - "Integration of optical-VHR and SAR data"

LIST OF ACRONYMS AND ABBREVIATIONS

ALTAM	ALTAMIRA Information
ASAR	Advanced SAR
CNR	Consiglio Nazionale delle Ricerche
COSMO-SkyMed	Constellation of Small Satellites for Mediterranean Basin Observation
DEM	Digital Elevation Model
DInSAR	Differential SAR Interferometry
DORIS	Ground Deformation Risk Scenarios: an advanced assessment service
DPC	Dipartimento di Protezione Civile
ELGI	Eötvös Loránd Geophysical Institute of Hungary
ENVISAT	Environmental Satellite
EO	Earth Observation
ERS	European Remote-Sensing Satellite
ESA	European Space Agency
EU	European Union
FOEN	Federal Office for the Environment
GAMMA	Gamma Remote Sensing AG
GBInSAR	Ground-based Interferometric Syntetic Aperture Radar
IGME	Instituto Geológico y Minero de España
InSAR	Interferometric Synthetic Aperture Radar
IPTA	Interferometric Point Target Analysis
IREA	Istituto per il Rilevamento Elettomagnetico dell'Ambiente
IUGS-WGL	International Union of Geological Science Working Group on Landslides
LOS	Line Of Sight
MHz	Megahertz
PGI	Polish Geological Institute
POLIMI	Politecnico di Milano
PREVIEW	PREVention, Information and Early Warning pre-operational services to support the management of risks
PS	Permanent/ Persistent Scatterer
PSI	Persistent Scatterers Interferometry
PSInSAR™	Permanent Scatterers Interferometry SAR
SAR	Synthetic Aperture Radar
SBAS	Small BAseline Subset

SPN	Stable Point Network
TRE	Tele-Rilevamento Europa
UNIFI	Università di Firenze
VHR	Very High Resolution
WP	Work Package

EXECUTIVE SUMMARY

In the DORIS project, Work package 3 (Value added research and technology development) is focused on innovative research initiative aimed at improving the exploitation of the existing capabilities of EO data and technological means to forecast and manage natural and human induced hazards and risks. WP3 is responsible to provide research and development support for the definition of innovative procedures to use EO data and technology to ground deformation assessment in agreement with the Users requirements. Furthermore WP3 is focused on the improvement of EO data exploitation for a downstream service.

This document describes the results of the integration of ground based and space born InSAR technology for landslides monitoring and how these results can be used to improve landslide forecasting models. These results could be applied to geohazards mapping in the framework of the Emergency Core Service.

Table of Contents

1. INTRODUCTION

DORIS intends to go beyond the state-of-the-art in the science and the technology currently used for the detection, mapping, monitoring and forecasting of ground deformations, at different geographical scales and in various physiographic environments. Significant improvements are expected from the application of GBRI technology and its integration with space-born SAR data.

Satellite and ground-based radar interferometry apply at different spatial and temporal scales. Satellite SAR frames cover areas up to 100 km · 100 km with resolutions of a few tens of meters. The passage rates of the present satellites over the same area range between 4 and 46 days. The area covered by a GBRI systems depends on the distance from the point of observation, but it is usually limited to a few hundreds of meters up to a few kilometers, corresponding to a patch-landscape scale. The GBRI systems can presently acquire an image up to about every 40 ms and they are consequently more suitable for faster slope movements which require a close series of successive measurements. Therefore, satellite data allow the monitoring of extremely or very slow movements only, whereas the GBRI device allows the assessment of moderate velocity landslides (Canuti et al., 2004; Metternicht et al., 2005). In addition, the spatial coverage of satellite images is limited by the peculiar SAR imaging geometry, with large mountainous areas masked by layover and shadow. A terrestrial radar system, on the other hand, can be placed also in front of steep walls which are in most cases not visible from space.

Because of the above-mentioned characteristics and differences, the integration of these techniques permits to obtain useful information. In particular, it is possible to realize a preliminary study by satellite, to analyse wide areas and have a global idea of the situation, and then focalise the attention on specific areas, recognised by satellite as the most interesting in terms of instability, where it is possible to conduct a more detailed study by the application of GBRI technique.

2. GBRI

GBRI is a powerful terrestrial technique widely used in engineering and in geology to detect the displacements of targets. This technique is based on the principles of radars and interferometry. Radar techniques are an example of active remote sensing: they emit energy in order to scan objects and areas whereupon a sensor detects and measures the radiation that is reflected or backscattered from the target. Detection of the movement of the target along the line-of-sight is achieved with the use of the interferometric phase processing (R. Bamler and P. Hartl, Synthetic aperture radar interferometry, Inverse Problems, 14: R1-R54, 1998; P. Rosen P., S. Hensley, I. Joughin, F. Li, S. Madsen, E.

Rodriguez and R. Goldstein, Synthetic aperture radar interferometry, Proceedings of the IEEE, 88(3): 333-382, 2000).

At the end of the last century, the first prototype of this terrestrial technology was elaborated by the Joint Research Center (JRC). The JRC achieved significant results with the design, implementation, and licensing of LISA for landslide monitoring (Tarchi et al., 2003; Casagli et al., 2010). This sensor is based on Vectorial Network Analyser (VNA), used to measure the complex impedance of the circuit at a given frequency, a coherent transmitting and receiving set-up, a mechanical guide, a PC based on data acquisition and a control unit (Tarchi et al., 1997).

The transmitter and the receiver are mounted beside one another in a quasi-monostatic configuration on a mechanical linear rail, which is computer controlled, synthesizing a linear aperture along the azimuth direction. Synthetic aperture radar (SAR) imaging, is a mature technology synthesizing an aperture bigger than the real one by exploiting the movement of the platform on which the antenna is mounted. This is one of the most advanced techniques used to generate high-resolution images even when optical systems cannot perform the task in a satisfactory manner (Tarchi et al., 1997).The high-frequency front-end is based on a coherent up and down frequency conversion and can perform measurements in the C and Ku bands (Rudolf and Tarchi, 1999). The processing includes a coherent SAR algorithm and interferometric techniques. LISA's acquisition time is not faster than a few minutes. Currently, LISA is still the most advanced tool for landslide monitoring, and its application to avalanche monitoring is being started. Ellegi-LiSALab company, on June 2003 obtained an exclusive licence to commercially exploit this technology from JRC.

In the last years, other different instruments have been realized , with the increase of microwave technologies. New versions of Linear SAR set-up have been realized, to improve frequency and stability capabilities (Noferini et al., 2005). This instrument (IBIS-L, IDS Company) is able to generate microwave signals at definite increasing frequencies sweeping a radiofrequency band.

Ground based interferometer has been realized by GAMMA, too (Wiesmann A., C. Werner, T. Strozzi and U. Wegmüller, Measuring deformation and topography with a portable radar interferometer, 13th FIG International Symposium on Deformation Measurements and Analysis and 4th IAG Symposium on Geodesy for Geotechnical and Structural Engineering, Lisbon, Portugal, May 12-15 2008; Werner C., A. Wiesmann, T. Strozzi and U. Wegmüller, Gamma's portable radar interferometer, 13th FIG International Symposium on Deformation Measurements and Analysis and 4th IAG Symposium on Geodesy for Geotechnical and Structural Engineering, Lisbon, Portugal, May 12-15 2008;Werner et al., 2008; C. Werner, A. Wiesmann, T. Strozzi, A. Kos and R. Caduff, The GPRI Multi-mode Differential Interferometric Radar for Ground-based Observations, Proceedings of the 9th European Conference on Synthetic Aperture Radar (EUSAR 2012), Nürnberg, Germany, 23 - 26 April 2012). This instrument uses real aperture antennas: one of them is used to transmit and two others to receive. The three antennas are mounted parallel to one another on a rigid high tower mounted on a precision rotational scanner. The azimuthally rotating of antennas about vertical axis

gives radar image. The vertical separation between the two receiving antennas permits the forming of a spacial interferometer, that is useful to measure height information (Strozzi, T., C. Werner, A. Wiesmann and U. Wegmüller, Topography Mapping With a Portable Real-Aperture Radar Interferometer, Geoscience and Remote Sensing Letters, 9(2): 277-281, doi: 10.1109/LGRS.2011.2166751, March 2012). Other components of the instrument are the scanners, a digital chirp generator, an analogue to digital converter, a computer and a microwave assembly, that contains the transmitter and two receivers. This technique uses Frequency Modulated-Continuous Wave (FM-CW) approach, that is well suited for near-range imaging. An image of GAMMA's portable radar interferometer is shown in Figure 1.

Figure 1 - *Picture of a radar interferometer showing the rotational scanner, antenna support structure, antennas and front-end and back-end microwave assembly.*

Another new generation of instrument is the Multiple-input and Multiple-output (MIMO) radar. This technique is based on the fact that independent signals are transmitted through different antennas, and that these signals, after propagating through the environment, are received by multiple antennas (Bliss and Forsythe, 2005). This system produces a resolution improvement, in fact MIMO system has larger number of degrees of freedom, because it can work with multiple simultaneous waveforms at multiple receivers (Wang et al., 2008). Specifically, MIMO SAR uses M orthogonal waveforms, each transmitted from different phase centres, and N received phase centres

(Sammartino et al., 2010; Tarchi et al., 2012). This is the substantial difference in respect to current SAR, because this one uses closely spaced antenna arrays, instead in new MIMO system at each of the receive phase centres, the received signals are matched filtered for each of the transmitted waveforms forming MxN channels (Wang, 2011). This instrument can be applied on satellite or on ground; here, in this elaboration, we have focused our attention on the ground based one. Following picture shows a scheme of MIMO SAR acquisition system (Fig. 2).

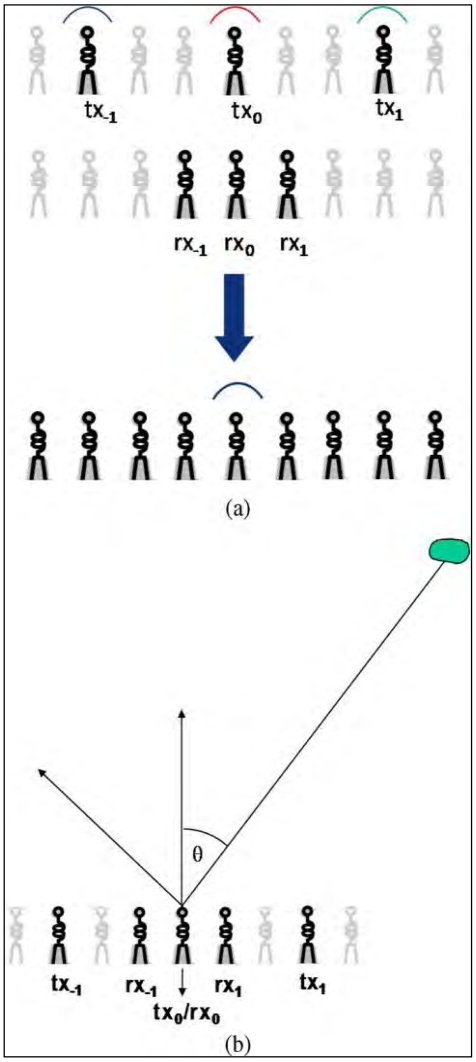

Figure 2 - *Sketches of MIMO configurations. (a) MIMO transmit array (top), receive array (middle) and equivalent Nyquist-spaced array with one element only transmitting (bottom); (b) MIMO geometry for deriving equations (Tarchi et al., 2012).*

3. INTEGRATION OF DINSAR AND GBRI

Differential SAR interferometry is generally carried out with the two-pass technique (Massonnet and Feigl 1998). Each scene pair has been co-registered and the associated coherence, phase and intensity matrix images have been generated for the entire satellite scenes frame. The spatial distribution of interferometric coherence was strongly affected by land use. Coherence zones in the same test site were generally variable over the different interferograms, in relation to the different baselines and temporal gap between scene pairs. To extract the phase component due to slope movements over coherent pixels, the topographic phase component is generally removed by projecting to SAR geometry external DEM. Atmosphere bias correction is carried out using a different applications and subtracted from the interferogram.

The integration of space-borne DInSAR and GBInSAR was experimentally applied in northern Italy during a research project aimed at testing the potentiality of the application of C-band space-borne interferometry and Ku-band ground based interferometry during different specific civil protection activities (Corsini et al., 2006). Main research objectives were the detection of the movements of complex earth and rock slides affecting built-up areas during the 1990s, and the near real-time monitoring of a reactivated rotational earth slide over an emergency period of 15 days. Results of space-borne interferometry did qualitatively fit with the geological interpretation of the mass movements and with ground truths such as damaged buildings and in situ monitoring systems (Corsini et al., 2006). However, this was not achieved in quantitative terms, suggesting that this technique should be used limitedly for displacement recognition and not monitoring. On the other hand, ground-based interferometry proved valuable both for a qualitative and a quantitative estimate of slope movements (Corsini et al., 2006).

3.1. Integration of PSI and GBRI

Limitations are mainly due to temporal and geometrical decorrelation and atmospheric artefacts (Colesanti et al., 2003 and references therein). Atmospheric noises produce strong spatial correlation within each individual SAR acquisition, but are uncorrelated in time. Contrariwise, target motion is generally correlated in time and it depends on the particular displacement phenomenon (Ferretti et al., 2001). Phase stable point wise targets, hereafter called Permanent Scatterers (PS), can be detected on the basis of a statistical analysis on the amplitudes of their electromagnetic returns (Ferretti et al., 2001). Atmospheric effects can be removed by combining data from long time series of SAR images and only targets (scatterers) slightly affected by both temporal and geometrical decorrelation should be selected (Ferretti et al., 2001).

Generally, the term Persistent Scatterers Interferometry (PSI) is usually employed to indicate all the multi-temporal techniques. The availability of huge historical SAR

archives confers to PSI the ability to measure and monitor "past deformation phenomena" (Crosetto et al. 2010). Different PSI procedures are described in the Deliverable 3.1.

Remote sensing monitoring systems based on PSI and GBInSAR can overcome most of the typical limitations of conventional monitoring techniques (geothecnical and topographic). Radar sensors can operate over wide areas in almost any weather conditions, continuously over a long time, providing real-time widespread information with millimetric accuracy without the need of accessing to the study area.

In order to evaluate the potential use of the integration of PSI and GBInSAR for landslides hazard mitigation, these methodologies have been applied at the Castagnola landslides (Liguria region, NW Italy). The analysis has been performed making use of set of ERS 1/ERS2 images acquired in 1992-2001 period. The outcomes of PSI analysis allows to confirm the landslide extension as mapped within the PAI (Hydrogelogical setting plan) and to define the time-series deformations and to reconstruct the past line-of-sight mean velocities of the landslide (Del Ventisette et al., submitted).

Following the high velocities detected by the PSI and the extensive damages surveyed in the buildings of the village, the GBInSAR monitoring system has been equipped during October 2008 and three distinct campaigns have been carried out until March 2009. The interpretation of the detected deformation allows to derive a multi-temporal deformation map of the landslide, showing the up-to-date displacement field and the mean landslide velocity. A new landslide boundary has been defined and two landslide sectors characterized by different displacement rates have been identified and the area affected by movements has been extended. Hence the new landslide hazard zonation obtained could be directly exploited as a new tool for appropriate planning and development (Del Ventisette et al., submitted).

4. RESULTS

In this section the considered phenomena which characterize each test site will be briefly described. Moreover the results obtained using the methodologies developed by the data providers are reported.

4.1. Messina Province, Sicily, Italy

4.1.1. *Considered phenomena*

Landslide hazard in the Messina Province (North-eastern Sicily, Italy) is mainly associated with instability phenomena in the Monti Nebrodi ridge, that is a 70 km long ridge with ENE-WSW direction and it is part of the Sicilian Apennines. Recent landslides affected the town of San Fratello, located to the west of the city of Messina.

The history of San Fratello is marked by historical landslide events such as the January 11th 1922, a landslide that caused hundreds of deaths in the town and about 10,000 people were evacuated (Guzzetti, 2000). On 13th and 14th February 2010, the east side of San Fratello was affected by a landslide of considerable size (about 1 km^2, according to preliminary estimates by the Regional Department of Civil Defense, Region Sicily (DRPC)). In the geographic position of San Fratello and a detail of an orthophoto of the studied area, with the first contouring of the landslide, are shown.

Figure 3 *- Geographic location of San Fratello and a detail of an orthophoto of the studied area, with the first contouring of the landslide (in red).*

The geomorphology of the area, with frequent slope breaks and many erosion forms, makes the area prone to these types of landslides, especially on lithologies characterized by poor mechanical properties, such as those outcropping in the zone. Intense and exceptional rainfall event was the main factor that, combined with the steep slopes,

triggered several slope movements along the Monti Nebrodi.

After the last event (February 13th, 14th 2010), a detailed study of the geology of the area has been conducted; it revealed the presence of a silt-clay overlay, with a thickness of about 10 m, above the clayey unit called Argille Scagliose Superiori and, locally, the presence of alternating sandstones and clays levels, belonging to the Frazzanò Flysch and the Monte Soro Flysch. Moreover, throughout the inhabited area, there is an aquifer, with depth between 0.5 and 2.5 meters.

4.1.2. *Procedure*

The displacements of the San Fratello landslide area have been studied pre- and post-event by InSAR techniques by satellite and by ground based systems. The satellites used were the ENVISAT, by ESA space agency, the RADARSAT-2, by Geospacial Services International, and the COSMO-SkyMed, by Italian Space Agency (ASI).

The data of ENVISAT and RADARSAT-2 have been used to analyze the situation pre-event, because these data cover a period between November 2003 and January 2010. The PS-InSAR elaboration of these data permitted to obtain information about the areas characterized by the highest displacements.

The COSMO-SkyMed data are representative of the post-event period: they have been acquired between May 2010 and May 2011. The PS-InSAR elaboration of these data permitted to compare the post-event displacements with the ones pre-event.

The data acquired by satellite have been integrated and compared with the ones obtained by GB-InSAR technique.

In fact a GB-InSAR instrument, a portable Linear SAR (LISA), was installed in San Fratello in March 2010; deformation maps have been realized using the data obtained by this system, and displacement time series of specific points on the landslide have been produced.

4.1.3. *Application of the procedure*

In the post-event, since March 10th 2010, the DRPC in collaboration with the Department of Earth Sciences of the University of Florence, installed a GB-InSAR. The system employed was designed and implemented by Ellegi-LiSAlab s.r.l. and JRC and installed on a stable support, in Sanguinera, that is located on the slope facing the San Fratello landslide, at an average distance of 3.3 km (Figure 4).

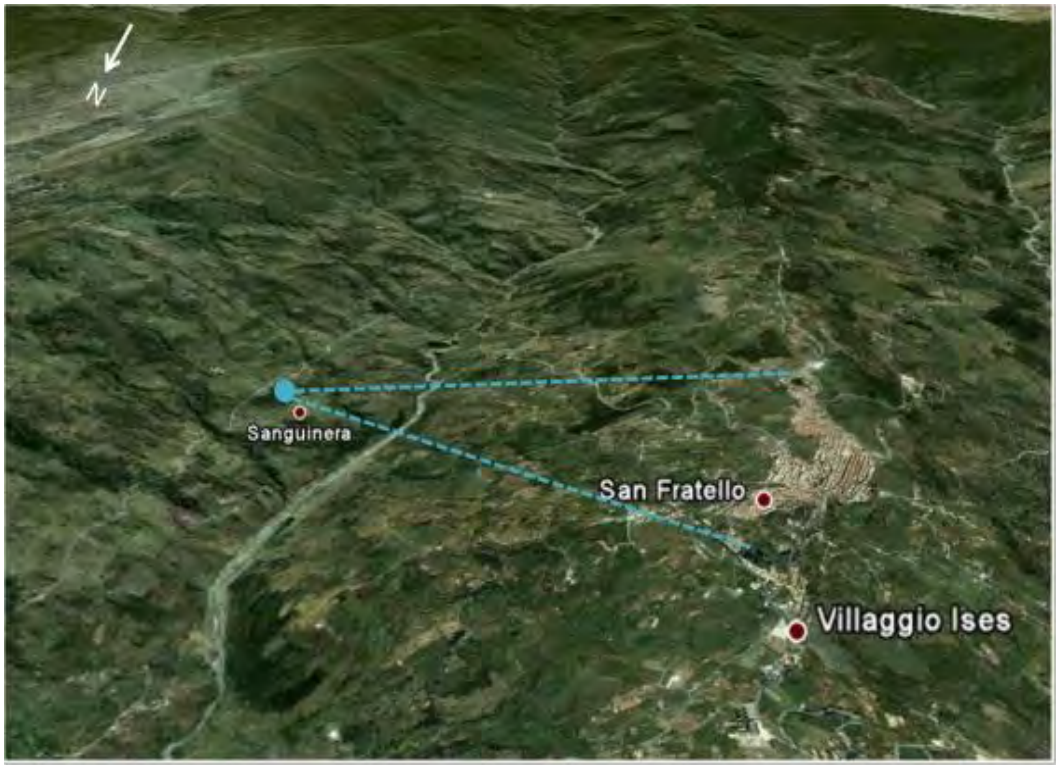

Figure 4 - *GB-InSAR position and its field of view.*

Monthly cumulative deformation maps were made through the interferometric radar data and the displacement time series of some representative points of the landslide were extracted and analyzed. An example of interferogram obtained during this campaign is shown in Figure 5. The colour of each pixel represents the LoS (line of sight) component of the displacement (Figure 6).

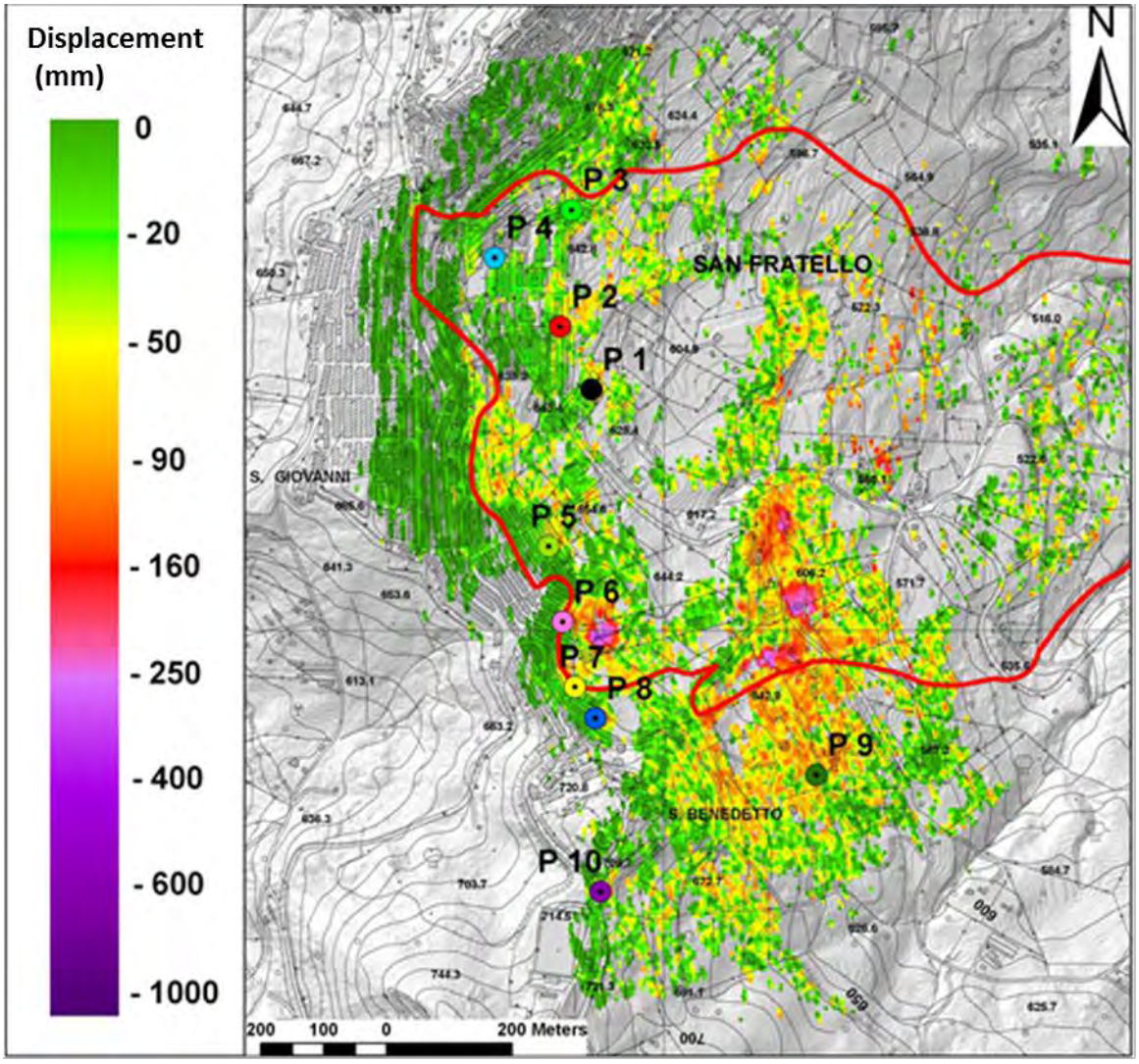

Figure 5 *- Example of a displacement map of the studied area.*

The interferogram in Figure 5 represents the displacements along the LoS, since monitoring (March 10th 2010) to May 31st 2011. It shows the presence of principal movements concentrated in defined areas, in the upper part of the slope. On the interferogram some representative points are displayed; the displacement time series of these points, obtained using the GB-InSAR data, are shown in Figure 6.

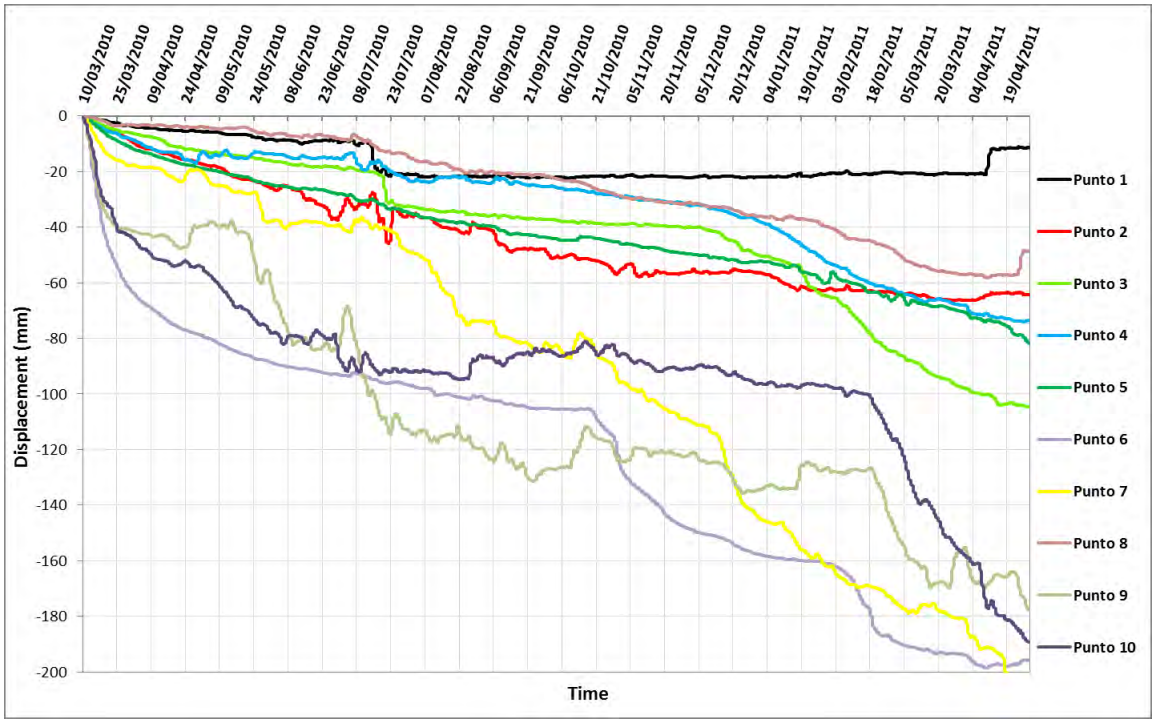

Figure 6 *- Displacement time series of ten representative points of the landslide area.*

The displacements were also studied by the analysis of data obtained through satellite interferometry (PS-InSAR). Especially the ENVISAT and RADARSAT-2 data stacks in descending and ascending orbits, and the COSMO-SkyMed in descending orbit were analyzed.

The ENVISAT satellite, provided by ESA space agency, works in C band with a repeat cycle of 35 days (Metternicht et al., 2005). The analyzed images regard data acquired between November 22nd 2003 and May 20th 2009.

Because of the acquisition mode and the exposition of the instable slope, the best information about displacement is obtained from data stacks in ascending orbits.

In Figure 6 the ENVISAT data, acquired in ascending orbit and elaborated with PS-InSAR technique, are shown.

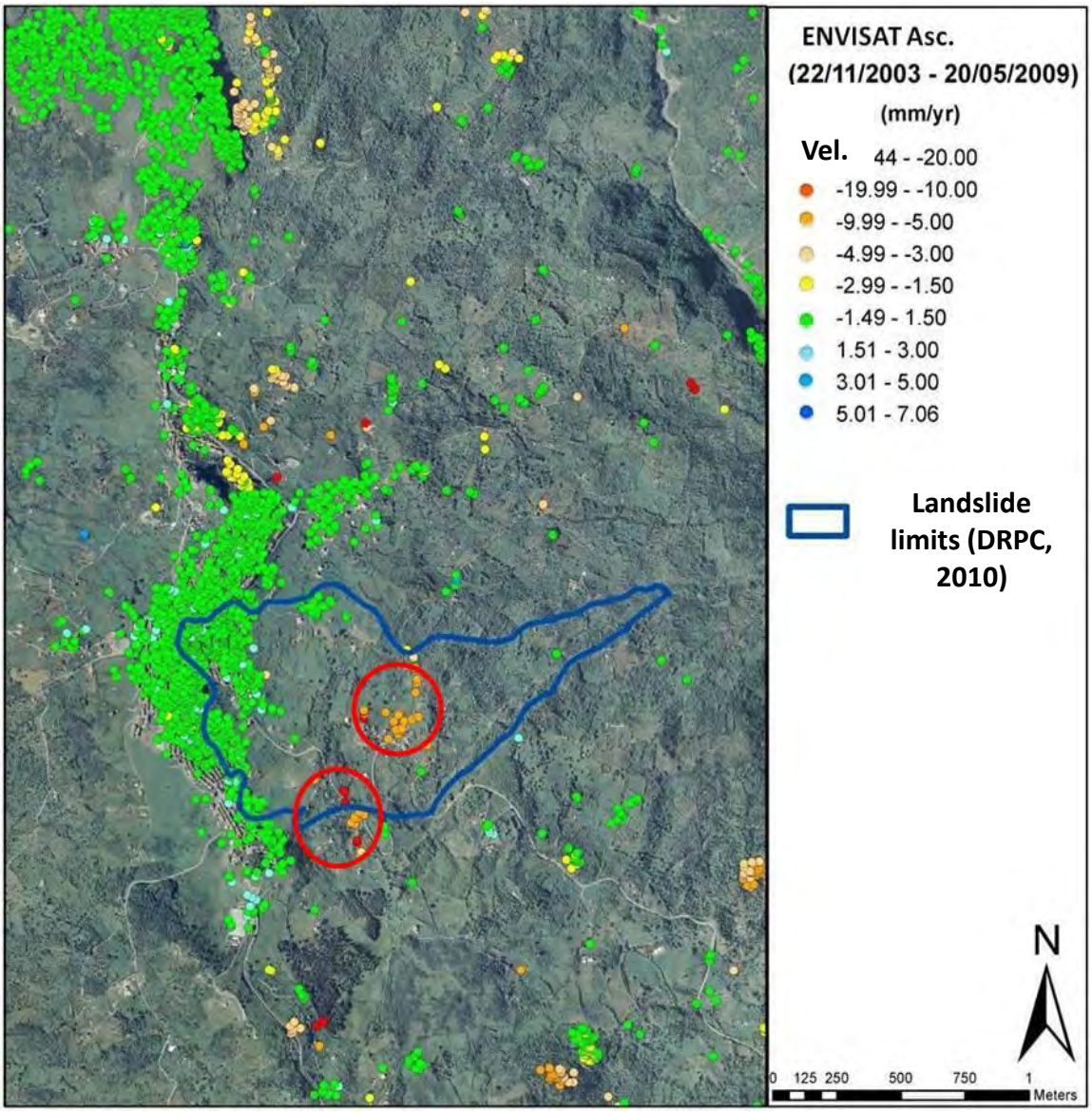

***Figure** 7 - PS ENVISAT, obtained by data acquired in ascending orbit. In red, the areas characterized by higher displacements are emphasized.*

The RADARSAT-2 satellite, provided by Geospacial Services International, works in C band with a repeat cycle of 24 days (Corsini et al., 2007). The analyzed images regard data acquired between December 30th 2005 and January 26th 2010.
The RADARSAT-2 data, acquired in ascending orbit and elaborated with PS-InSAR technique, are shown in Figure 8.

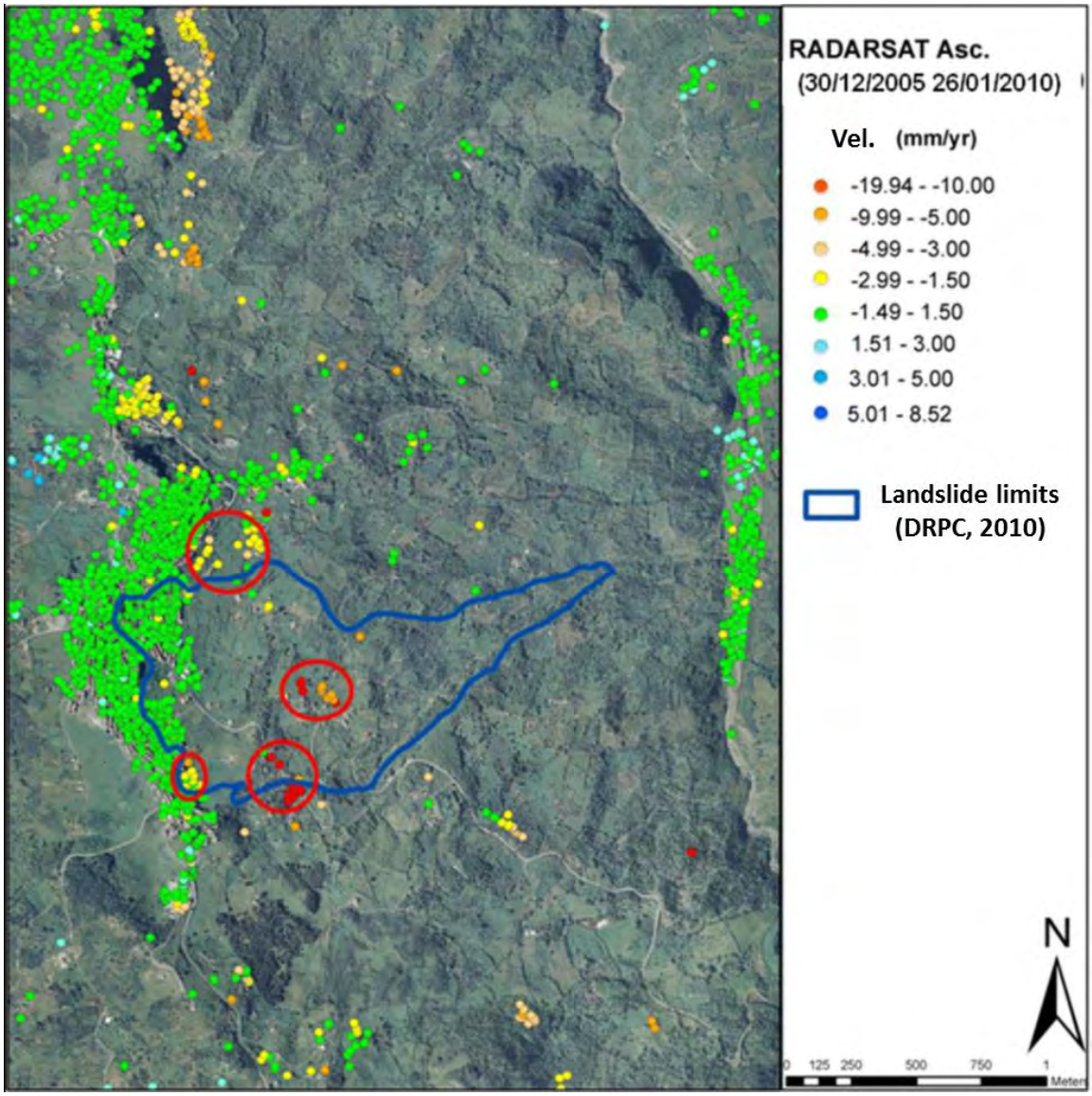

Figure 8 *- PS RADARSAT, obtained by data acquired in ascending orbit. In red, the areas characterized by higher displacements are emphasized.*

The areas marked in red in 8 and Figure *8*9 show the presence of movements in correspondence of landslide region, before the landslide triggers.

COSMO-SkyMed is commissioned and funded by Italian Space Agency (ASI) and Italian Ministry of Defense, a system that consists of a constellation of four Low Earth Orbit mid-sized satellites, operating at X-band, with a repeat cycle of 16 days (www.cosmo-skymed.it). The analyzed images regard data acquired between May 16th 2011 and May 2nd 2012.

The COSMO-SkyMed data acquired in ascending orbit and elaborated with PS-InSAR technique, are shown in 8.

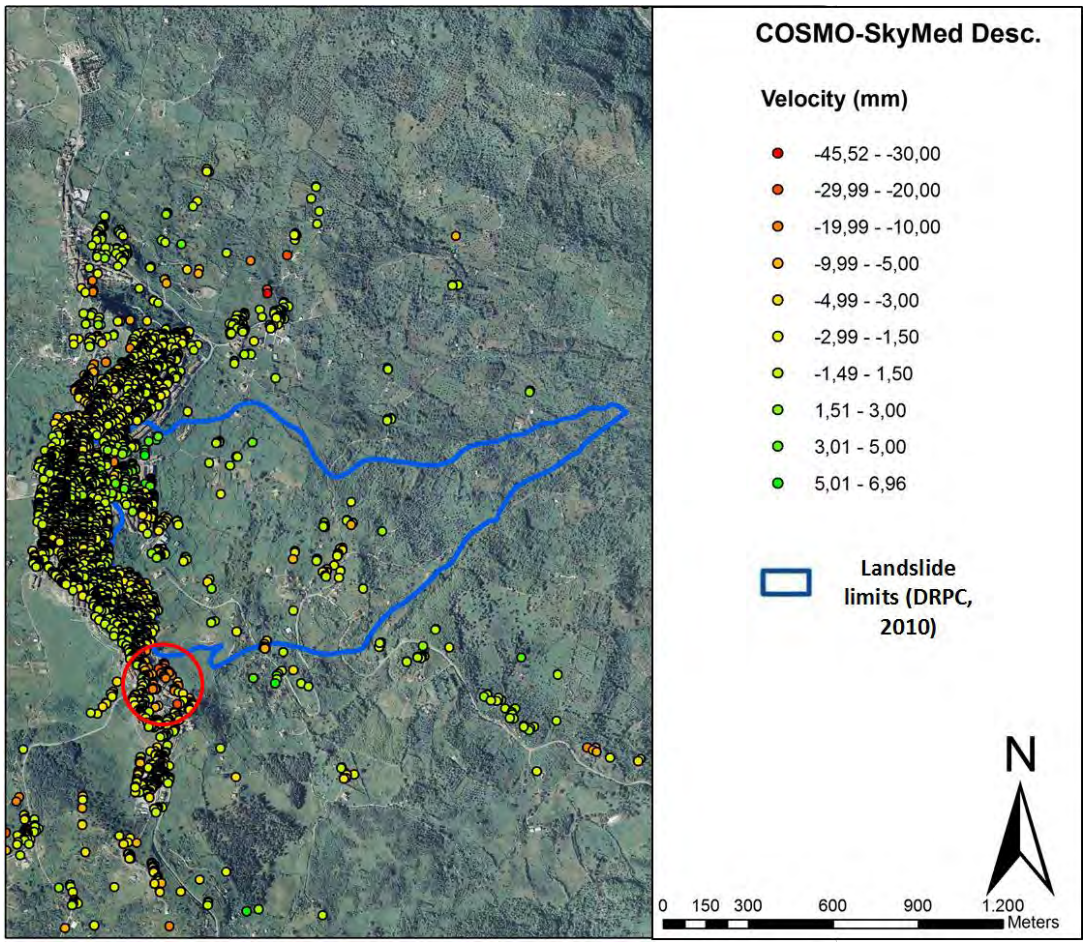

Figure 9 *- PS COSMO-SkyMed, obtained by data acquired in descending orbit. In red, the areas characterized by higher displacements are emphasized.*

The COSMO-SkyMed data are representative of a period post-event. The PS analysis shows the presence of some displacements, that are registered, in the same period, by GB-InSAR too. In particular, in , the area characterized by higher movements is emphasized.

The integration of GBInSAR and PSInSAR techniques permitted to demark the areas characterized by higher displacements and to propose a new contouring of the landslide, whose extension was re-evaluated being around 1.2 km^2 (Figure 9).

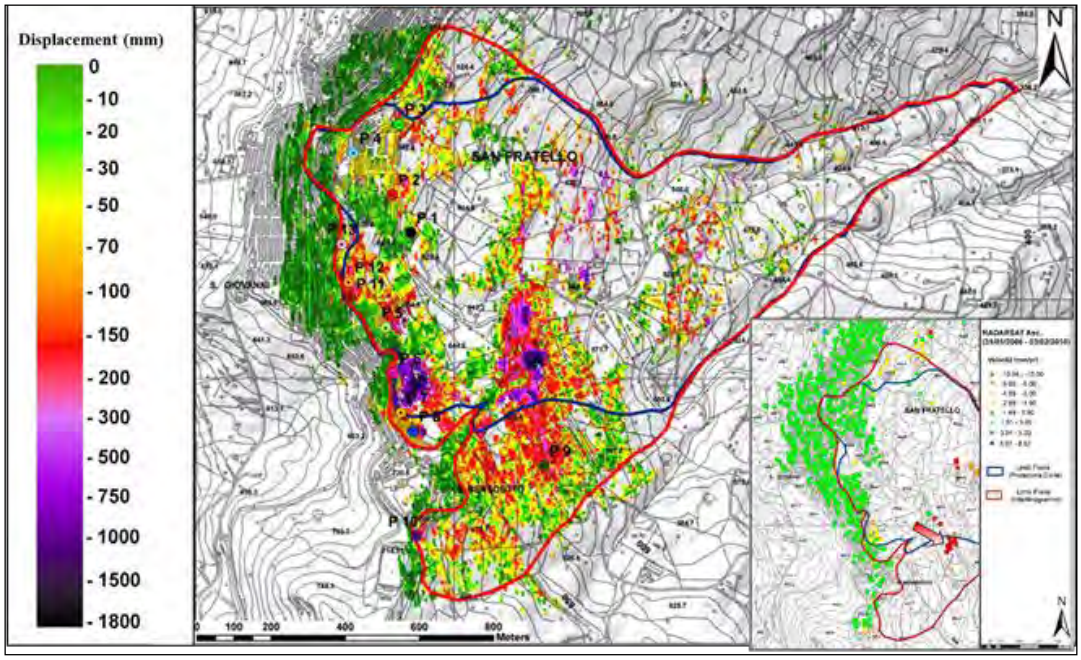

Figure 9 *- Propose of a new contouring of the landslide (in red), outlined by the results of GB-InSAR and PS-InSAR campaigns.*

The integration of the techniques also permitted to confirm the presence in the area of paleo-landslides, as outlined also by historical data, and by the IFFI and PAI archives. The studies permitted also to conclude that the landslide of San Fratello is a complex movement, which has certainly affected the land cover and that the geomorphological features, together with the geology and the presence of an aquifer close the surface, represented the main predisposing factors.

4.2.The Portalet case study (Central Pyrenees, Spain)

We have chosen the results obtained in Portalet landslide (Central Pyrenees, Spain) because the methodology proposed for the integration of multi-sensor radar data and the implemented hydro-geomechanical finite element model that reproduces the kinematic

behavior of very slow landslides are applicable to any other similar landslides of the selected test sites in DORIS project.

4.2.1. *Considered phenomena*

The study area is located in the upper part of the Gállego River valley in the Central Spanish Pyrenees (Sallent de Gállego, Huesca) close to the Formigal ski resort. This is a structurally complex area, outcrops of Paleozoic material of Gavarnie mantle were affected by the Hercynian folding phases and the alpine tectonics. Pyrenean deglaciation and widespread structural relaxation shaped the landscape triggering complex landslides that have been previously described and mapped by various authors (Bixel et al. 1985, García-Ruíz et al. 2004). We focus our work on two of these landslides developed on the southwest-facing hillside of Petrasos Peak: the "Portalet landslide" and "Petruso landslide" (landslides 2 and 5 in Fig. 11). These landslides are rotational slide earth flows, 30 to 50 meters thick. The mobilized materials involve sands and gravels found within a clayey matrix with sandstone levels, greywackes and shales. A subsequent third earth flow can be recognized in the north part of the Portalet landslide (landslide 1 in Fig. 11). Nowadays, rock falls and avalanches are still occurring in the main scarps. Recent small landslides triggered by river erosion can also be found on the toe of the main landslides.

In summer 2004, the excavation of the foot of the slope carried out to build a parking area (black line in Fig. 1) reactivated the existing slide surfaces generating a new small earth slide called the "Parking landslide", 380 m long and 290 m wide (landslide 4 in Fig. 11). The occurrence of this new local landslide prevented the digging to be finished and affected the connection road to France. Constructive solutions were carried out to stabilize the hillside involving re-profiling of the landslide toe, building of small retaining walls and drainage systems. However, field observations indicate that the landslide is still moving.

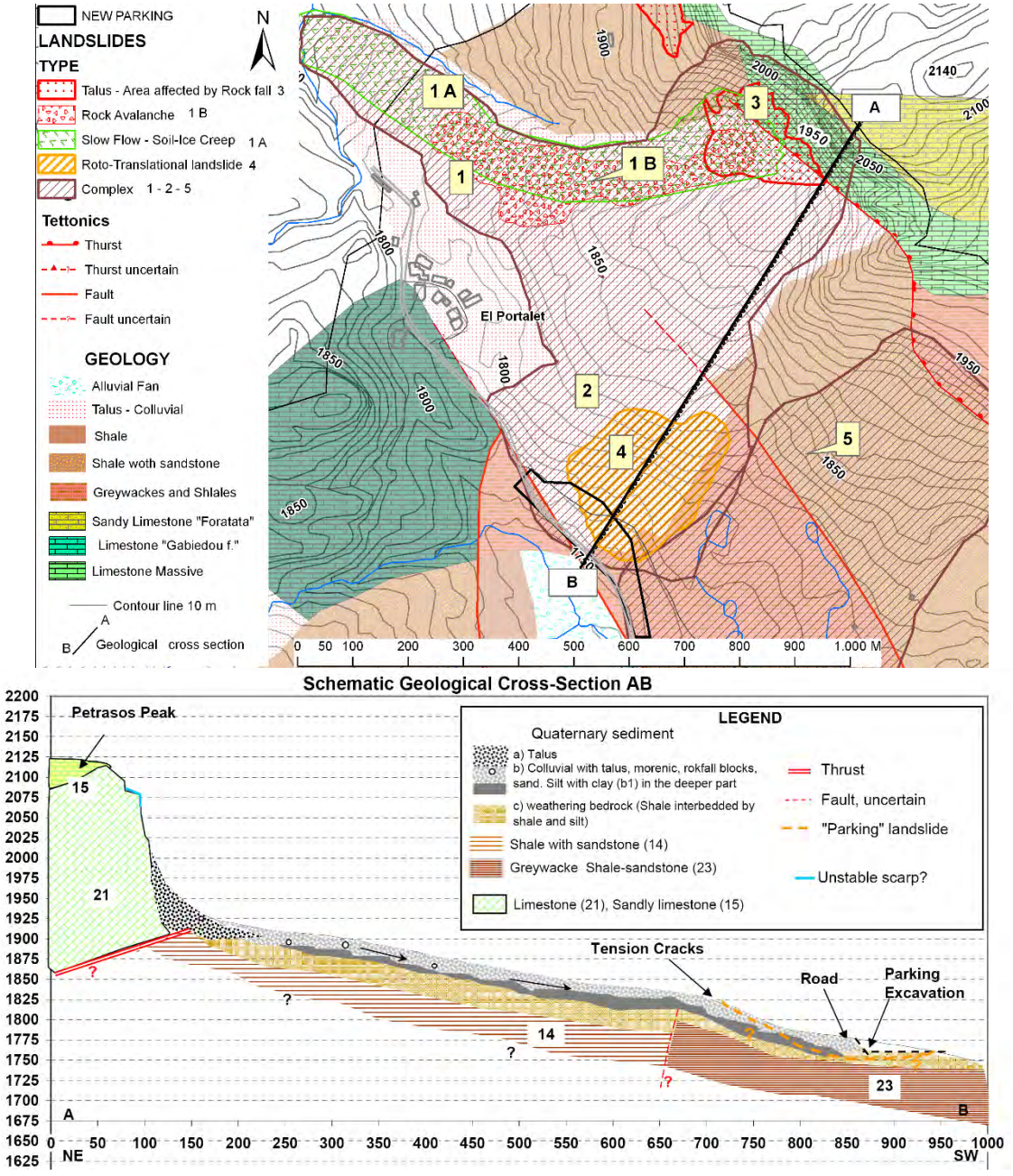

Figure 11 *- Geomorphological and geological sketch of the Portalet landslides area and cross section AB.*

4.2.2. *Procedure*

The displacements of the Portalet landslide area have been studied by radar satellite and ground based systems. The combination of multi-sensor data has been useful to differentiate different landslide displacement directions, to measure different velocity

patterns within the same moving mass, and to distinguish the slower (natural) and faster (human induced) landslides (Herrera et al., 2012). The projection along the steepest slope of LOS displacements reduces the geometrical differences introduced by the acquisition geometry of each satellite.

In a second stage this information was used to implement an hydro-geomechanical finite element model that reproduces the kinematic behavior of this large very slow landslide. The time dependent analysis reproduces the acceleration and deceleration of the moving mass due to hydrological changes, permitting to model a 2 meter displacement for the past eight years that coincides with monitoring data (Fernández-Merodo et al., 2012).

The GB-SAR sensor was installed at a distance of about 600 m from the main body of the landslide on a hill overlooking the parking area. It kept working continuously for 47 days, from the 5 October to the 21 November 2006, providing displacement map of the illuminated area at a rate of 1 per hour (Herrera et al., 2009).

The SPN SB approach was used to process 43 SAR images acquired by ERS-2 and ENVISAT satellites from July 2001 to September 2007; 14 SAR images acquired between May and October 2008 by the TerraSAR-X satellite (Herrera et al., 2010); and 12 SAR images recorded between December 2006 and March 2010 by ALOS PALSAR (L-band) satellite. Note that the time span covered by the X-band images is less than 1 year, whereas temporal coverage of ALOS and ERS&ENVISAT acquisitions are around 3 and 4 years, respectively. In order to compensate the topographic component of the interferomeric phase a 15 m resolution DEM generated by the Cartographic Service of the Government of Aragón (Spain) was used. The level of multi-looking applied, the maximum spatial and temporal baseline, and the number of generated interferograms for the different bands can be found in Table 1.

Band	L	C	X
Wavelength [cm]	23	5,8	3
Incidence angle	38	23	45
Angle between azimuth and North	13.7	14.5	12.83
Orbital track	664	237	124
Acquisition mode	Fine beam	Image mode	Strip map
Resolution in azimuth [m] & range [m]	3.5 x 4.7	4 x 8	1.9 x 0.9
Minimum temporal span between two	46	35	11
Max. theoretical velocity [mm/yr]	460	150	250
Temporal span	12/06-03/10	07/01-09/07	05/08-11/08

Number of SAR images	12	43	11
Number of interferograms	42	163	55
Multi-look operation	8 x 8	10 x 2	4 x 4
Maximum spatial baseline [m]	4000	800	400

Table 1.

4.2.3. *Application of the procedure*

The integration of multi-temporal and multi-SAR data has allowed us to detect and monitor different ground surface displacements and their temporal variations associated to each of the slope movements present in the El Portalet landslide complex (Fig. 12)

Landslide 1: the good PS coverage is due to the large amount of large limestone blocks mantling the landslide and the western orientation (N232E), which favours PS detection for descending orbit satellites. The measured Vlos projected in the steepest slope is 15 mmyr^{-1} with C (2001-2007) and X (2008) bands (Fig. 12b and12c).

Landslides 2 and 4: in the summer of 2004, the excavation at the foot of landslides 2 and 5 induced the development of a secondary failure in the lower part of landslide 2 (4 in Fig. 11) and accelerated landslide 5. After the completion of amelioration measures, Herrera et al. (2009) measured displacement rates as high as 1184 mm yr-1 with a ground based SAR (GB-SAR) that was validated with D-GPS measurements (Fig. 12b). Detecting displacement by means of DInSAR using satellite images was unfeasible because the velocity was too fast for PS detection. However, in the area situated above the crown of this secondary failure, both X- and L-band PS measured Vslope values between 30 and 97 mmyr-1 (Fig. 12c and 12d). These values can be explained as an indication of the retrogressive effect of landslide 4 related to the loss of lateral confining pressure in the head scarp. Concerning landslide 2, the three bands measure Vlos values between 11 and 14 mm yr-1, which are close to the 24 mm yr-1 rate measured by D-GPS for the 2006-2011 period (Fig. 12a).

Landslide 5: consistently with the D-GPS measurements, average Vslope of 29 and 21 mm yr-1 was measured from L- and X-band PS, respectively (Fig. 12c and 12d). The poor PS coverage is due to the predominance of low grass and the absence of large boulders at the surface. Overall, the available data indicate that the activity of this landslide complex (up to 360 mmyr-1) is responsible for the damages observed both on the A-136 road and the parking lot in the2008-2010 period.

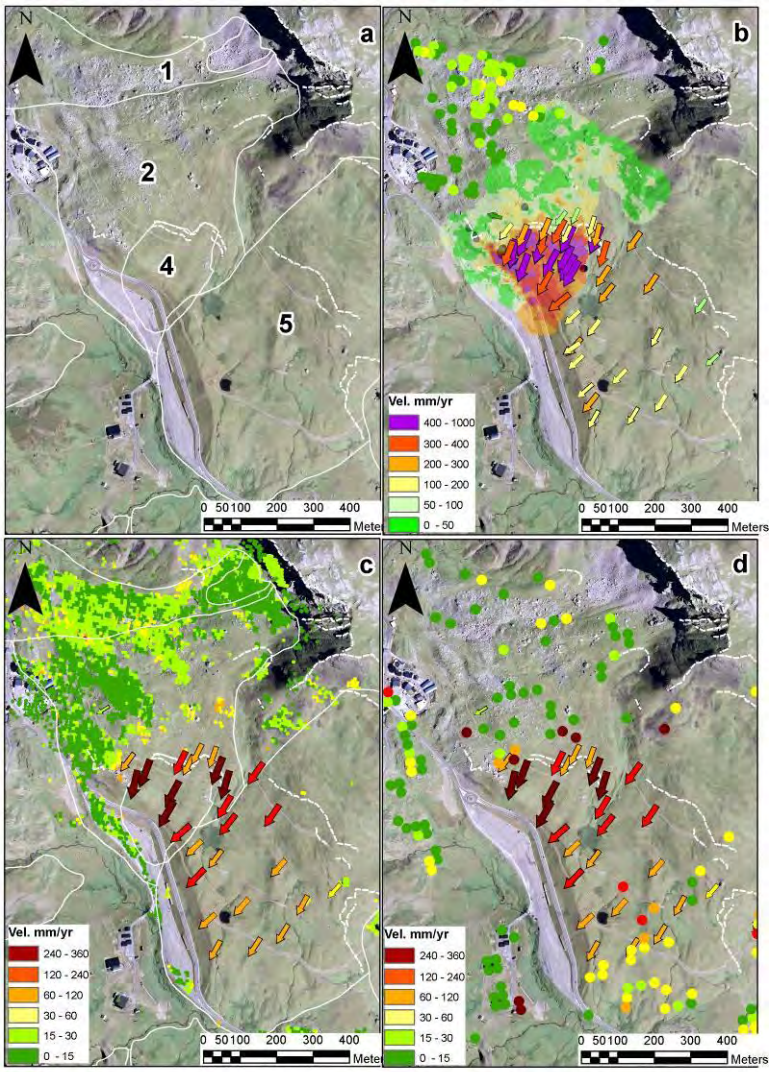

Figure 12 *- a) Portalet landslide area; b) Measured Vslope from C-band (2001-2007), GB-SAR (2006) and D-GPS (2006); c) Measured Vslope from X-band (2008) and D-GPS (2006-2011); c) Measured Vslope from L-band (2007-2010) and D-GPS (2006-2011).*

In the second stage of this procedure monitoring data has been used to implement an hydro-geomechanical finite element model that reproduces the kinematic behavior of this large very slow landslide. The interaction between solid skeleton and pore fluids is modeled with a time dependent u-p_w formulation and a groundwater model that takes into account recorded daily rainfall intensity. A viscoplastic constitutive model based on Perzyna's theory is applied to reproduce soil viscous behavior and the delayed creep deformation. The time dependent analysis reproduces the acceleration and deceleration of the moving mass due to hydrological changes. Overall the model has reproduced a 2

meter displacement in the past eight years that coincides with in-situ monitoring data (Figs. 13 and 14).

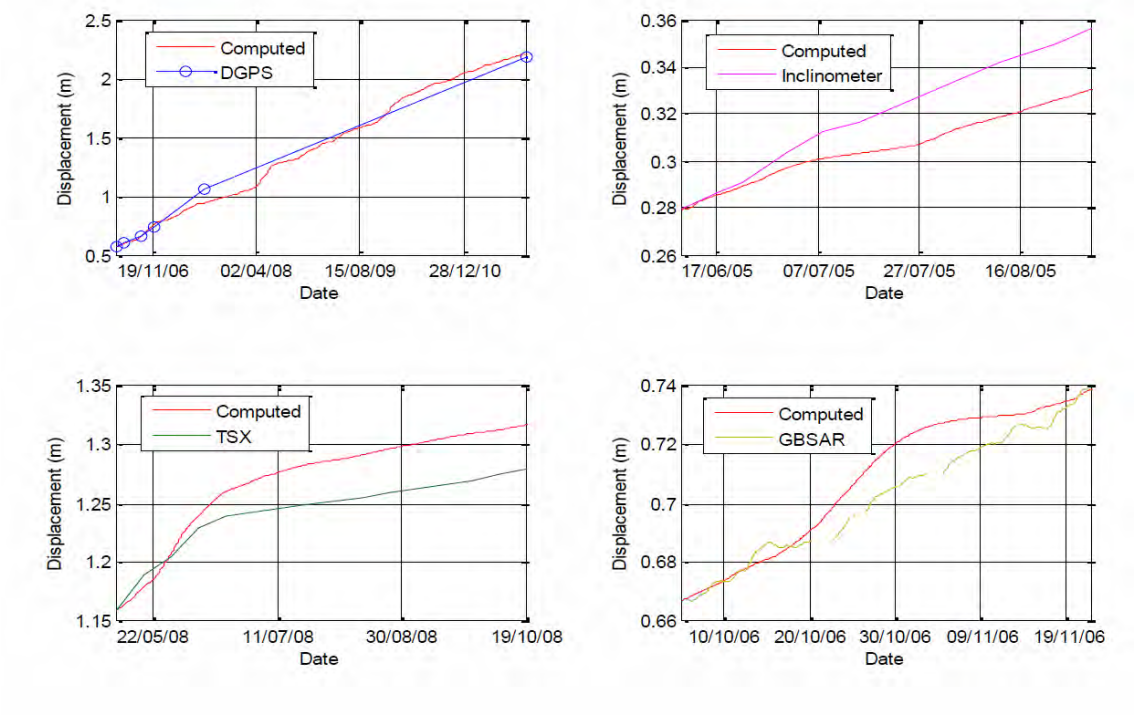

Figure 13 *- Computed and measured mid-slope displacement*

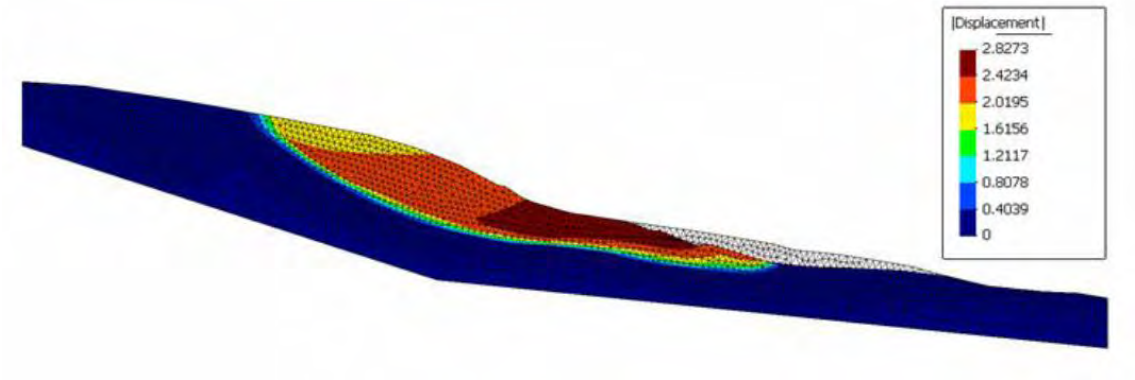

Figure 14 *- Computed displacement in m (2005-2011)*

4.3. Zermatt (VS), Switzerland

4.3.1. *Considered phenomena*

The Mattervalley in the Swiss Alps starts from Visp at the bottom of the Rhonevalley up to the famous station of Zermatt (Fig. 15). In this valley there are numerous instable slopes, including some densely populated regions prone to landslides. There are also many installations for touristic purposes in the unstable slopes, sometimes located in the permafrost areas. Many landslides, rockslides, and rockfalls are still active and there are high annually costs for the mitigation and countermeasures. The damage concerns inhabited areas, touristic installations and many roads. For the Mattervalley a landslide monitoring is not available, but several of the large landslides are known and the geological documents will allow an integration of the radar interferometric techniques for hazard assessment. Due to the high costs related to landslide activity and to the difficulties in the detection of the active, slow or dormant portions of the landslide, the use of a radar interferometric approach can positively impact on the current practices used by the local authorities to carry out the hazard mitigation activities.

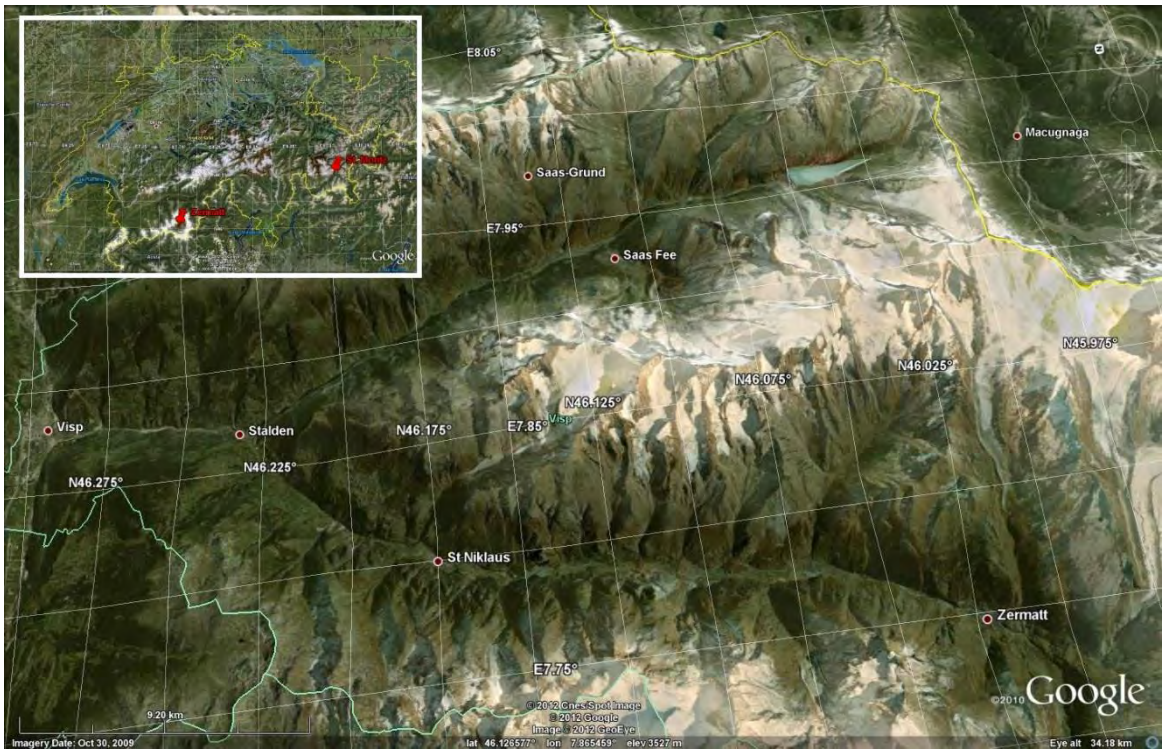

Figure 15 *- Geographic location of Zermatt and the Mattervalley in the Swiss Alps.*

Permafrost creep leads to the formation of rockglaciers, which are large masses of ice/rock debris mixture acting as conveyors of debris on mountain slopes. Numerous active rockglaciers are found in the Mattervalley above 2200 to 2500 m a.s.l. Their deformation rate ranges typically between 0.1 and 2.0 m/yr. The velocity of rock glaciers has risen significantly since the 1980s over the whole alpine range in response to a significant permafrost warming. Recently, destabilized (or "surging") rockglaciers showing morphological indices of landslide-like mass wasting (e.g. development of transversal cracks, surface subsidence of the upper section, rapid advance of the front position) that affects the terminal part or the whole of the landform have been reported from several regions in the European Alps, including Grosse Grabe, Gugla, Dirru and principally Grabengufer in the Mattervalley (Fig. 16). Currently, the detection of the state of activity of these very rapid moving rockglaciers is hardly feasible with satellite SAR data, because of signal decorrelation after the 46, 35 and 11 day repeated intervals of the ENVISAT, ALOS and TerraSAR-X satellites, respectively. The role of space-borne radar interferometry as an element in a warning system is thus insignificant for these very rapid landslides, but an in-situ radar imaging system can overcome some of the limitations of satellite systems.

Also particularly significant in the Mattervalley site is a large deep seated gravitational slope deformation on the upper Breithorn west face. Breithorn is a 3'178 m high peak above the alpine hiking trail connecting Grächen to Zermatt. The area is dominated by gneissic rocks belonging to the crystalline Mischabel unit [T. Labhart, *Geologie der Schweiz*, 6th Edn., Ott Verlag, Thun, 211 pp., 2004]. Debris originating either from the weathering of the bedrock or from various gravitational processes (e.g. rockslides, rockfalls) are covering the bedrock in many places. A considerable part of the area, particularly above 2500 m a.s.l., is characterized by slopes without any vegetation or dominated by scarce patches of alpine grass. The coherence on satellite SAR interferograms is therefore generally well preserved on a monthly time scale.

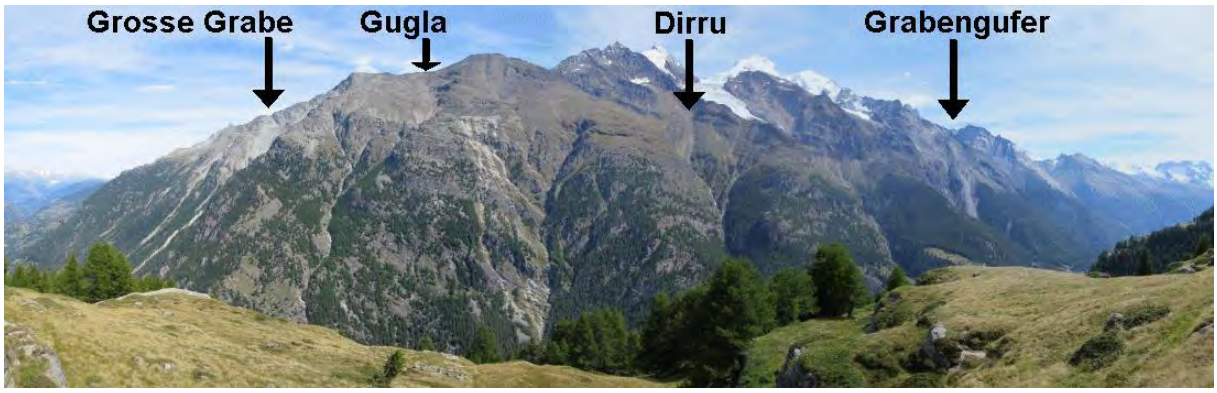

Figure 16 *- Orographic right side of the Mattervalley from the GBRI position on September 2, 2010 with indication of the most active rock glaciers. The Breithorn landslide is located just on the left (i.e. north) of the Gugla rockglacier.*

4.3.2. *Procedure*

Ground-based radar measurements of the orographic right side of the Mattervalley were performed from a position on the opposite side of the valley (Fig. 17). The distance to the target was considerably large, from about 3 km to more than 5 km, with significant atmospheric artefacts. Measurements were performed in six campaigns with the Gamma Portable Radar Interferometer:

→ 1-3 September 2010,

→ 11-12 October 2010,

→ 10-12 August 2011,

→ 16-17 August 2011,

→ 23-24 August 2011,

→ 30-31 August 2011.

In order to study the effect of the large distance to the objects, two campaigns of the Grabengufer rockglacier were also performed on July 20 and 21, 2010 and August 10, 2011 from a distance of about 1 km.

Interferograms of every campaign were processed in series and cumulative displacement maps of the fastest moving objects were computed for the six dates. In addition, displacement maps of the slower moving objects were computed using a few image of every campaign. In all cases, the interferograms were filtered to remove noise and atmospheric disturbances. Geocoding was performed using a high-resolution DEM with a posting of 2 m.

Figure 17 *- GBRI position and its field of view (i.e. backscattering intensity image).*

The displacement of the Mattervalley was studied using the following satellite SAR data:

Satellite	Band	Time period	Number of scenes	Nominal repeat cycle
ERS-1/2 SAR	C-band	1995 - 2000	31	35 days
ENVISAT ASAR	C-band	2002 - 2010	29	35 days
JERS-1 SAR	L-band	1993 - 1996	11	46 days
ALOS PALSAR	L-band	2007 - 2010	4	44 days
TerraSAR-X	X-band	2008 - 2012	47	11 days
Cosmo-SkyMed	X-band	2008 - 2011	23	16 days
Radarsat-2	C-band	2010	3	24 days
ERS-1	C-band	1991	31	3 days

A PSI processing was performed using the ERS-1, ERS-1/2 SAR, ENVISAT ASAR, and TerraSAR-X data sets. In addition, differential interferograms were computed using a large number of image pairs, including a Cosmo-SkyMed pair with 4 days time interval.

4.3.3. *Application of the procedure*

The scans performed with the terrestrial radar system during the various campaigns with a time interval between subsequent acquisitions on the order of 30 minutes were interfered in series and cumulative displacement maps were computed. We measured the highest rates of movement for the Grabengufer rockglacier, with values larger than 10 cm/day in 2010 and on the order of 10 cm/day in 2011. This is in agreement with measurements performed with other surveying techniques like GPS and tachometers over this rockglacier which since the beginning of 2009 shows a landslide-like mass wasting phenomenon. The comparison with the Grabengufer rockglacier measurements from a distance of about 1 km shows the degradation of the azimuth resolution of the terrestrial radar system, but nevertheless similar rates of movement.

The same displacement map shown before but represented with a different color scale highlights the movement of the three other active rockglaciers of our test area, i.e. Grosse Grabe, Gugla and Dirru (Fig. 18). General rates of movements of these rockglaciers at the front were larger than 1 cm/day. Also visible in these images is the movement of the Hobärg glacier.

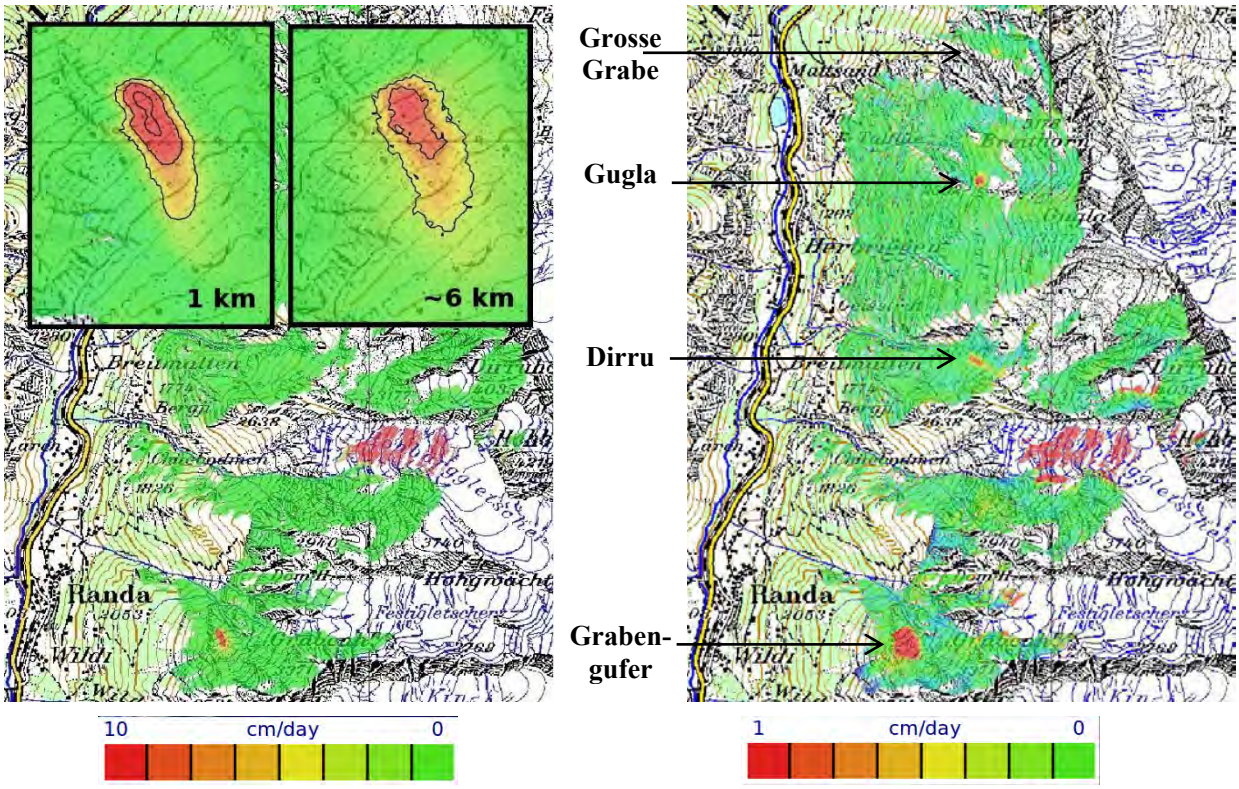

Figure 18 *- Displacement map from terrestrial radar interferometry for the 1 to 3 September 2010 measurements with different color scales. The inset shows an enlargement for the Grabengufer rockglacier (right) and a comparison with a measurement from a closer location on 20 July 2010 (left).*

The activity of these very rapid moving rockglaciers cannot be detected from satellite SAR interferometry. Interferograms with short perpendicular baselines from JERS-1 and Cosmo-SkyMed (Fig. 19), but also from TerraSAR-X and ENVISAT ASAR (not shown here), present all very important signal decorrelation after the 44, 4, 11 and 35 days repeat intervals of these SAR sensors operating at L-, X- and C-band, respectively. On the other hand, with all these satellites, other slower moving landslides can be well discriminated.

In order to quantitatively study the movement of the slower landslides, PSI analyses were conducted with the summer TSX images of 2009 and 2011 (Fig. 20). The image shows all points detected with these two separate analyses and the comparison with the ground-based radar interferogram computed with images of August 10 and 16, 2011. In both the ground-based and the satellite-based results the signals of the Breithorn landslide to the north of the Gugla rockglacier and of the landslide just to the north of the Grabengufer rockglacier are very well visible. Other smaller signals scattered along the test-site and consistently observed in the two cases can be appreciated as well. In spite of the very different viewing geometries the rate and the shape of the detected signals is very similar from ground and satellite.

PSI analyses conducted with ERS-1/2 and ENVISAT images might be finally used to detect the slowest moving landslides, where rates of movement are below a couple of cm/yr (Fig. 21). All the areas with movement rates larger than these values appear without information, similarly to vegetated regions and slopes affected by layover and shadow. The spatial coverage with valuable information around the Breithorn landslide is larger on the ERS-1/2 solution than on the ENVISAT one, suggesting an acceleration during more recent years.

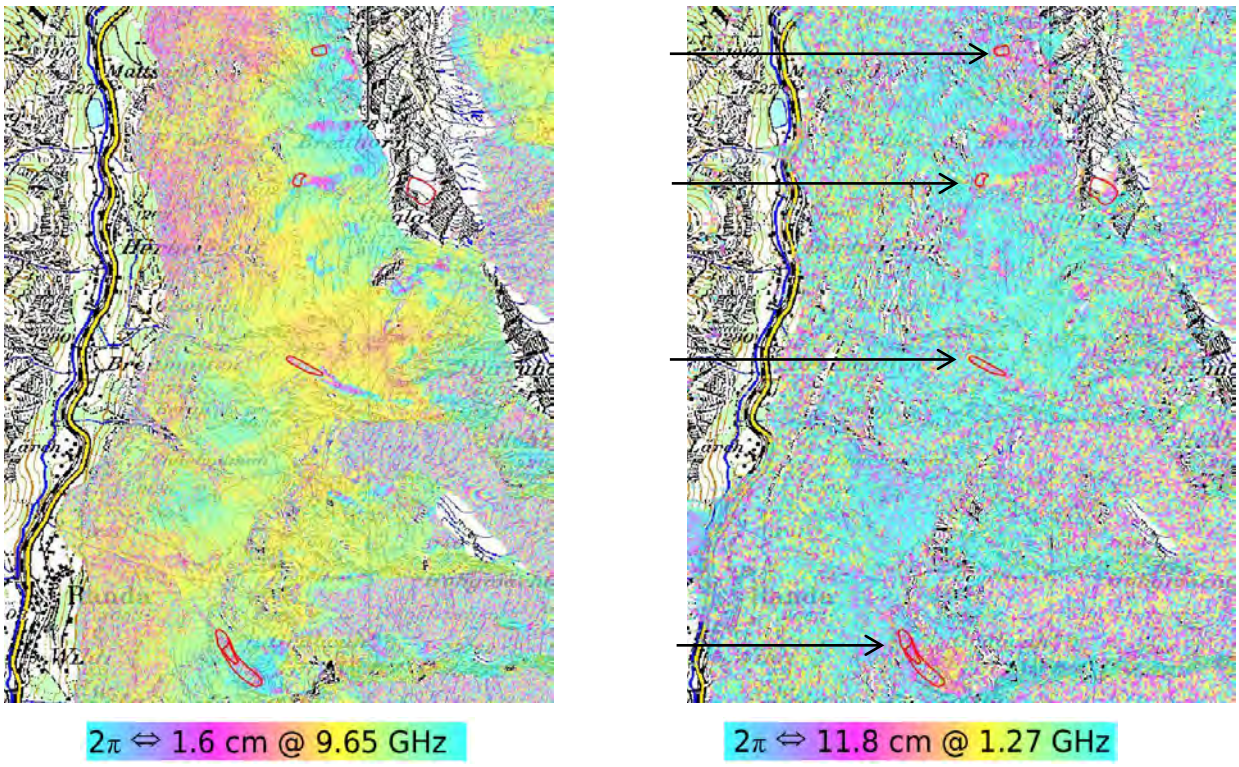

Figure 19 *- Cosmo-SkyMed differential interferogram from 23 to 27 September 2011 (4 days, 28 m, left) and JERS-1differential interferogram from 22 June to 18 September 1996 (88 days, 120 m, right).*

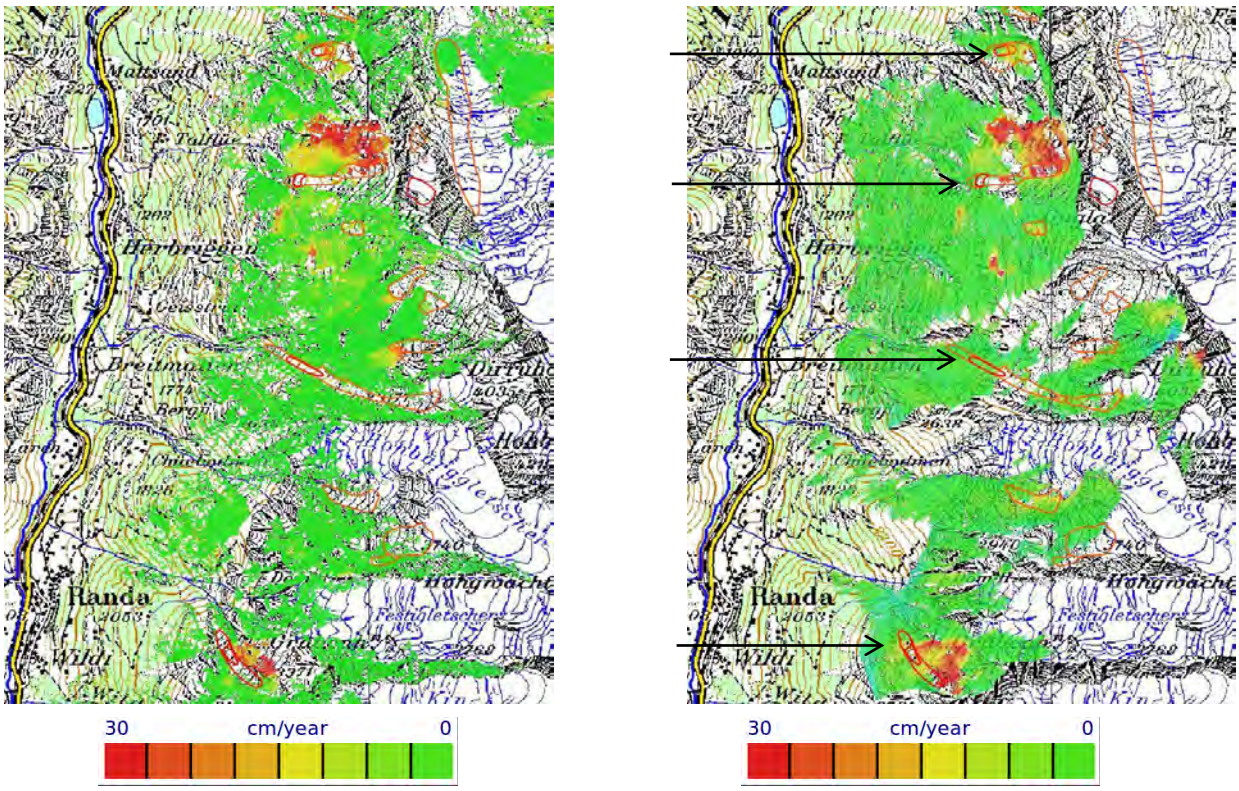

Figure 20 *- Displacement map from (left) TerraSAR-X PSI using only summer images of 2009 and 2011 and (right) terrestrial radar interferometry with acquisitions from August 10 to 16, 2011.*

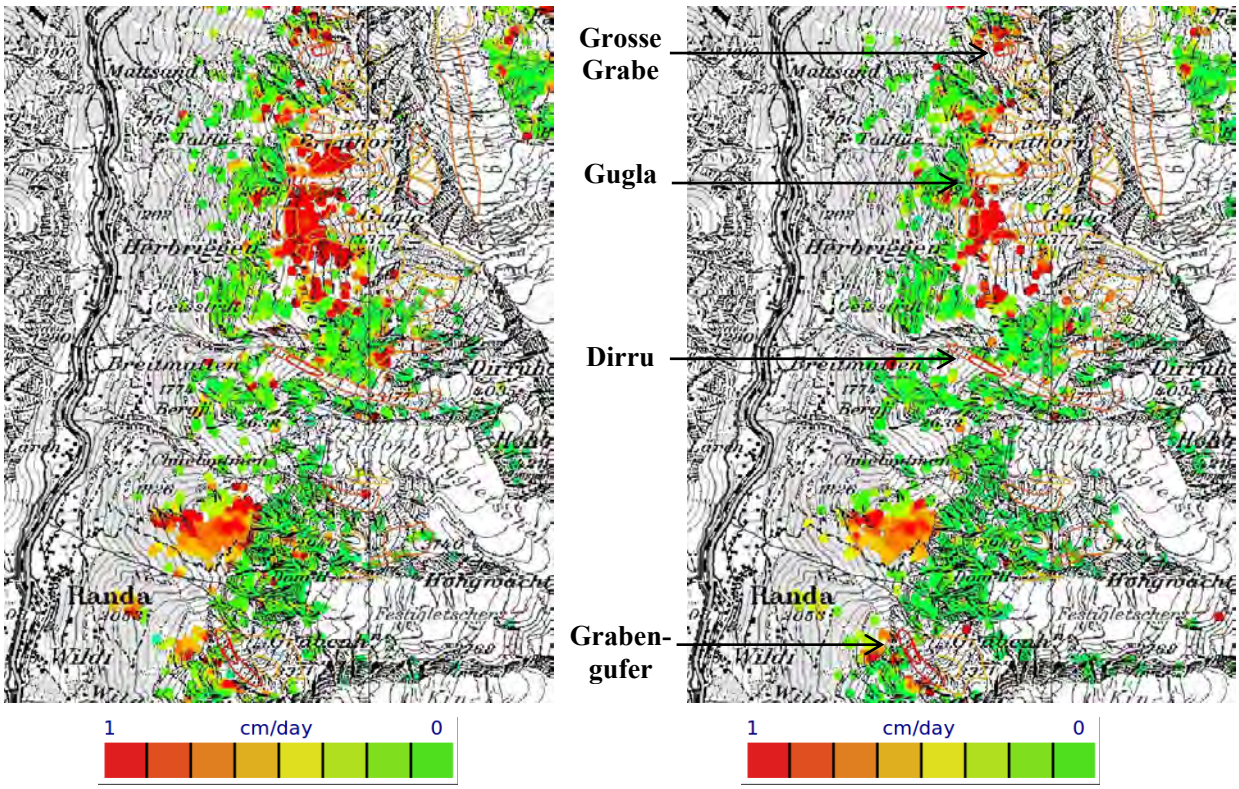

Figure 21 *- Mean displacement rates from (left) ERS-1/2 PSI and (right) ENVISAT PSI.*

REFERENCES

Bliss D.W. and Forsythe K.W. 2003. "Multiple-input multiple-output (MIMO) radar and imaging: Degrees of freedom and resolution," in *Proc. 37th Asilomar Conf. Signals, Syst. Comput.*, Pacific Grove, CA, Nov., 1, pp. 54–59.

Canuti, P., Casagli, N., Ermini, L., Fanti, R., & Farina, P. 2004. Landslide activity as a geoindicator in Italy: Significance and new perspectives from remote sensing. *Environmental Geology*, 45, 7, pp. 907–919.

Corsini, A., Farina, P., Antonello, G., Barbieri, M., Casagli, N., Coren, F., Guerri, L., Ronchetti, F., Sterzai, P., Tarchi, D., 2006. Spaceborne and ground-based SAR interferometry as tools for landslide hazard management in civil protection. *International Journal of Remote Sensing,* 27, 12, pp. 2351–2369.

Crosetto M, Monserrat O, Iglesias R, Crippa B (2010) Persistent scatterer interferometry: potential, limits and initial C- and X-band comparison. *Photogramm. Eng. Remote Sens*., 76, 9, pp. 1061–1069.

Fernández-Merodo, J.A., García-Davalillo, J.C., Herrera G., Mira, P., Pastor, M., 2012. 2D viscoplastic finite element modelling of slow landslides: the Portalet case study (Spain). Submitted to *Landslides*.

Guzzetti F. 2000. Landslide fatalities and evaluation of landslide risk in Italy. *Engin. Geol.*, 58, pp. 89–107.

Herrera, G., Notti, D., García-Davalillo, J., Mora, O., Cooksley, G., Sánchez, M., Arnaud, A., and Crosetto, M., 2011, Analysis with C- and X-band satellite SAR data of the Portalet landslide area: *Landslides*, v. 8, p. 195-206.

Herrera, G., Fernández-Merodo, J.A., Mulas, J., Pastor, M., Luzi, G., Monserrat, O., 2009. A landslide forecasting model using ground based SAR data: The Portalet case study. *Engineering Geology* 105: 220–230

Herrera, G., Gutiérrez, F., García-Davalillo, J.C., Guerrero, J., Notti, D., Galve, J.P., Fernández-Merodo, J.A., Cooksley, G., 2012. Multi-sensor advanced DInSAR monitoring of very slow landslides: the Tena Valley case study (Central Spanish Pyrenees). Submitted to *Remote Sensing of the Environment*.

Massonnet, D., Feigl, K.L., 1998. Radar interferometry and its application to changes in the Earth's surface. *Rev. Geophys.*, 36.

Metternicht,G.,Hurni, L.,Gogu, R., 2005.Remote sensing of landslides: an analysis of the potential contribution to geo-spatial systems for hazard assessment inmountainous environments. *Remote Sensing of Environment,* 98, pp. 284–303.

Noferini L, Pieraccini M, Mecatti D, Luzi G, Atzeni C, Tamburini A, Broccolato M (2005) Permanent scatterers analysis for atmospheric correction in ground-based SAR interferometry. *IEEE Trans. Geosci. Remote Sens.,* 43, 7, pp. 1459–1471.

Sammartino, P. F.Baker, C. J., Griffiths, H. D., 2010. Range-angle dependent waveform. *Proc. IEEE Radar Conf.*, 2010, pp. 511–515.

Tarchi, D., Ohlmer, E., Sieber, A.J., 1997. Monitoring of structural changes by radar interferometry. *Res. Nondestruct. Eval.*, 9, pp. 213– 225.

Tarchi, D., Leva, D., Casagli, N., Fanti, R., Luzi, G., Pieraccini, M., Pasuto, A., Silvano, S., 2003. Landslide monitoring by using ground-based SAR interferometry. An example of application to the Tessina landslide in Italy. *Eng. Geol.*, vol. 68, no. 1/2, pp. 15–30.

Tarchi, D., Oliveri, F., Sammartino, P.F., 2012. MIMO Radar and Ground-Based SAR Imaging Systems: Equivalent Approaches for Remote Sensing. *IEEE Commun. Mag.*, DOI 10.1109/TGRS.2012.2199120.

Wang, F. Ghosh, A. Sankaran, C. Fleming, P. Hsieh, F. and Benes S. J. 2008. "Mobile WiMAX systems: performance and evolution," *IEEE Commun. Mag.*, 46, no. 10, pp. 41–49.

Werner C., Strozzi T., Wesmann A., Wegmuller U. 2008. Gamma's portable radar interferometer. *13th FIG Symposium on Deformation Measurements ad analysis, LNEC*, Lisbon May 12-16 2008.